

## Process-based indicators to assess storm induced coastal hazards

Óscar Ferreira, Theodoros A. Plomaritis, Susana Costas

CIMA/FCT, University of Algarve, Campus de Gambelas, 8005-139, Faro, Portugal;  
oferreir/tplomaritis/scotero@ualg.pt

Corresponding author: Óscar Ferreira (oferreir@ualg.pt)

### Abstract

Storms are responsible for several hazards (e.g. overwash, erosion, inundation) in coastal areas, leading to the destruction of property and loss of life in populated areas. Various indicators are used to express potential storm impact and describe the associated hazards. The most commonly used indicators include either forcing parameters (e.g. wave height, sea level) or coastal morphologies (e.g. dune height or berm width). Whereas they do not represent the processes associated with storm induced hazards in coastal areas. Alternatively, a hazard could be better characterised if process-based indicators are used instead. Process-based indicators express the result of the forcing mechanisms acting over the coastal morphology and reflect both hydrodynamic and morphological characteristics. This work discusses and synthesizes the most relevant process-based indicators for sandy shores subject to overwash, erosion and inundation promoted by storms. Those include: overwash depth, potential and extent; shoreline, berm or dune retreat; vertical erosion; and inundation depth and extent. The selection of a reduced set of process-based indicators to identify coastal hazards induced by storms in sandy coasts will facilitate comparison of different coastal behaviours for distinct storm return periods, and help to optimise coastal management plans, thereby contributing to the reduction of coastal risks.

# 1 Process-based indicators to assess storm induced 2 coastal hazards on sandy coasts

3 Óscar Ferreira, Theocharis A. Plomaritis, Susana Costas

4 CIMA/FCT, University of Algarve, Campus de Gambelas, 8005-139, Faro, Portugal;  
5 oferreir/tplomaritis/scotero@ualg.pt

6 Corresponding author: Óscar Ferreira (oferreir@ualg.pt)

## 7 8 Abstract

9 Storms are responsible for several hazards (e.g. overwash, erosion, inundation) in  
10 coastal areas, leading to the destruction of property and loss of life in populated areas.

11 Various indicators are used to express potential storm impact and describe the  
12 associated hazards. The most commonly used indicators include either forcing  
13 parameters (e.g. wave height, sea level) or coastal morphologies (e.g. dune height or  
14 berm width). Whereas they do not represent the processes associated with storm  
15 induced hazards in coastal areas. Alternatively, a hazard could be better characterised  
16 if process-based indicators are used instead. Process-based indicators express the  
17 result of the forcing mechanisms acting over the coastal morphology and reflect both  
18 hydrodynamic and morphological characteristics. This work discusses and synthesizes  
19 the most relevant process-based indicators for sandy shores subject to overwash,  
20 erosion and inundation promoted by storms. Those include: overwash depth, potential  
21 and extent; shoreline, berm or dune retreat; vertical erosion; and inundation depth

60  
61  
62 22 and extent. The selection of a reduced set of process-based indicators to identify  
63  
64 23 coastal hazards induced by storms in sandy coasts will facilitate comparison of  
65  
66  
67 24 different coastal behaviours for distinct storm return periods, and help to optimise  
68  
69 25 coastal management plans, thereby contributing to the reduction of coastal risks.  
70

71  
72 26

73  
74  
75 27 Keywords: indicators; hazards; storms; overwash; inundation; erosion  
76  
77

78 28

## 79 80 81 29 1. Introduction 82

83  
84 30 Storms impacting sandy coastal areas produce hazards such as erosion and inundation  
85  
86 31 that, in turn, promote risk to life and property damage in occupied areas, and the  
87  
88  
89 32 alteration and/or fragmentation of habitats. Recent examples include the severe  
90  
91 33 coastal erosion and associated destruction of property caused by Hercules storm  
92  
93 34 (January 2014) that impacted the southwest coasts of France and England (Castelle et  
94  
95  
96 35 al., 2015; Masselink et al., 2016a,b); the inundation and loss of life caused by the  
97  
98 36 Xynthia storm (February/March 2010) in western France (e.g. Bertin et al., 2012); the  
99  
100 37 vast destruction caused by the superstorm Sandy (October/November 2012), in the  
101  
102 38 coastal mid-Atlantic states of the USA (Bennington and Farmer, 2015; Clay et al., 2016),  
103  
104 39 or by hurricane Katrina (August 2005), at the Gulf coast of the USA (Link, 2010;  
105  
106  
107 40 Kantha, 2013). Potential coastal damages and risks are expected to increase in the  
108  
109 41 near future not only in association with climate change (e.g. sea level rise, change in  
110  
111 42 frequency and magnitude of storms) but also due to increasing human occupation in  
112  
113  
114 43 coastal areas (Neumann et al., 2015).  
115  
116  
117  
118

119  
120  
121 44 Indicators, as a metric for coastal state, dynamics, behaviour or hazard, are a  
122  
123 45 straightforward way to express complex data and information and can therefore be an  
124  
125 46 important tool in the dialog among stakeholders (Carapuço et al., 2016). They are  
126  
127  
128 47 often based on a parameter that is used to characterise a coastal area. Coastal hazard  
129  
130 48 indicators are commonly used to express the potential storm impacts in coastal areas,  
131  
132 49 helping to identify and prioritise vulnerable regions (Nguyen et al., 2016). Storm  
133  
134 50 related hazards have been expressed in the literature by a large number of different  
135  
136 51 indicators that have been recently synthesised by the review works of Carapuço et al.  
137  
138 52 (2016) and Nguyen et al. (2016). For coastal erosion and flooding hazards Carapuço et  
139  
140 53 al. (2016) identified (and recommended) the use of several geoindicators, like  
141  
142 54 *shoreline/baseline position, shoreline evolution, beach/barrier elevation or beach*  
143  
144 55 *slope*. Nguyen et al. (2016) synthesized the existing indicators in literature related to  
145  
146 56 storm surge-driven flooding and coastal vulnerability and included geoindicators (e.g.  
147  
148 57 *coastal slope, geomorphologic characteristics*), hydrodynamic indicators (e.g. *wave*  
149  
150 58 *height, tidal range, surge height*) and coastal evolution indicators (e.g. *erosion rate,*  
151  
152 59 *shoreline/coastline position*). The aforementioned indicators, which represent a  
153  
154 60 summary of the ones that have been widely used and referred to in the international  
155  
156 61 literature, include forcing/driver parameters, coastal morphology characteristics and  
157  
158 62 even coastal evolution. It is, however, not clear how to select the most representative  
159  
160 63 parameter for a given hazard. The most commonly used parameters describe either  
161  
162 64 the driving mechanisms or the coastal morphology, rarely integrating both or fully  
163  
164 65 representing the processes associated with storm induced hazards in coastal areas.  
165  
166 66 Moreover, these indicators hardly differentiate relevant time-scales (or return periods)  
167  
168  
169  
170  
171  
172  
173  
174  
175  
176  
177

178  
179  
180 67 and/or values that are averaged over time, which can cause difficulties (and  
181  
182 68 exaggerated simplicity) in their application.

183  
184  
185 69 To fully characterise a coastal hazard it is necessary to use a set of indicators that  
186  
187  
188 70 combines the forcing mechanism and its effect on the coastal morphology, i.e.  
189  
190 71 process-based indicators. The majority of the indicators found in the literature cannot  
191  
192 72 be considered process-based. Process-based indicators can only be obtained from the  
193  
194 73 application of models that incorporate physical forcing mechanisms and that include  
195  
196 74 realistic coastal morphology elements, resulting in a parameter or set of parameters  
197  
198 75 that express the effects of the processes acting on the coastal system.

200  
201  
202 76 This work reviews and synthesizes the most relevant process-based coastal indicators  
203  
204 77 that can be applied for sandy coasts subject to storm-induced coastal hazards. The  
205  
206 78 main hazards assessed are: overwash, inundation, and erosion. The main goal is to  
207  
208 79 propose a set of process-based indicators that can serve as a reference for coastal  
209  
210 80 hazard studies on sandy shores. The rationale for using process-based indicators is  
211  
212 81 described in section 2. The definition, discussion and selection of indicators for each  
213  
214 82 analysed coastal hazard are detailed in section 3. Section 4 provides a synthesis of the  
215  
216 83 proposed indicators and their applicability, based on the use of simple parameters  
217  
218 84 highly representative of coastal hazards. Final considerations on current limitations  
219  
220 85 and future use of process-based indicators at sandy coasts are discussed in section 5.

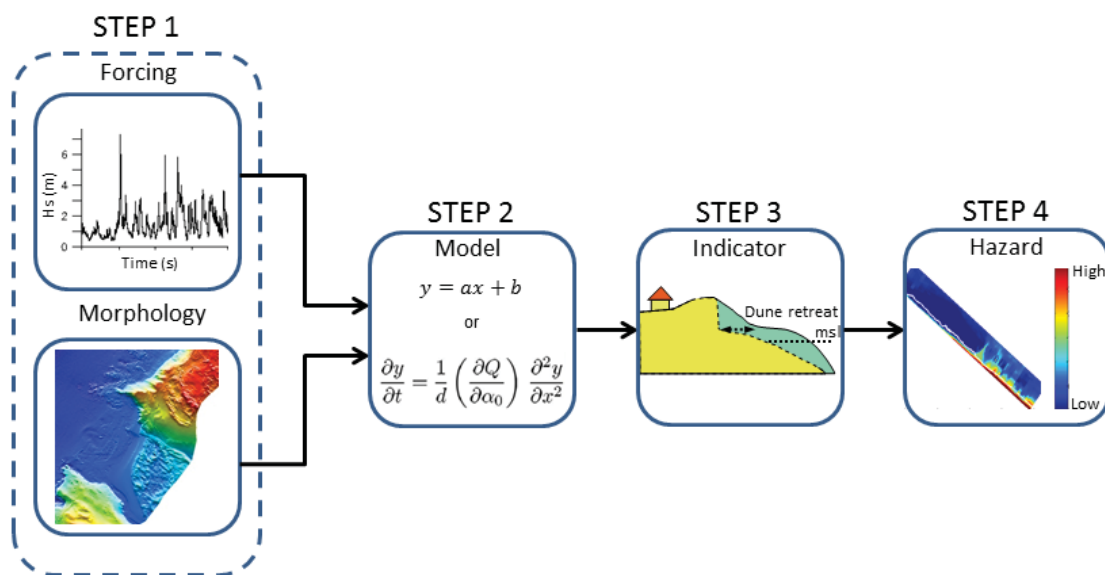
221  
222  
223  
224  
225 86

226  
227  
228 87 2. Process-based indicators  
229  
230  
231  
232  
233  
234  
235  
236

237  
238  
239  
240  
241  
242  
243  
244  
245  
246  
247  
248  
249  
250  
251  
252  
253  
254  
255  
256  
257  
258  
259  
260  
261  
262  
263  
264  
265  
266  
267  
268  
269  
270  
271  
272  
273  
274  
275  
276  
277  
278  
279  
280  
281  
282  
283  
284  
285  
286  
287  
288  
289  
290  
291  
292  
293  
294  
295

88 The vast majority of recommended coastal hazard related indicators in the literature  
89 (see reviews by Bush et al., 1999; Carapuço et al., 2016; Nguyen et al., 2016) only take  
90 into account: (i) the characteristics of the physical/morphological features of the  
91 coastal system, or (ii) the driving mechanism. Combinations between both,  
92 representing the processes and the consequent hydrodynamic or morphological  
93 results (process-based indicators), are not commonly used and have not yet been the  
94 subject of a synthesis. Process-based indicators are directly related to hazard and  
95 represent the interaction between driving mechanisms and the coastal morphology.  
96 The process-based indicators are therefore obtained by using formulations or models  
97 (from simple to complex) that will combine the driving mechanisms (e.g. storm  
98 parameters like wave height, wave period, storm duration or sea level) and the coastal  
99 system morphology (such as beach face slope, dune height, berm width, grain size or  
100 bathymetry) (Figure 1, steps 1 and 2). The result will be an impact (e.g. erosion,  
101 overwash occurrence) that can be expressed through an indicator that has a physical  
102 meaning (e.g. flood depth, shoreline retreat). Overall, results can be reclassified into  
103 new classes that express different levels of hazard according to stipulated  
104 limits/thresholds allowing an illustrative mapping of the hazard (Figure 1, steps 3 and  
105 4). These thresholds can be defined locally or regionally, allowing a comparison of the  
106 hazard intensity within a specific coastal area and also between different coastal areas.  
107 Furthermore, such indicators can often be used to estimate (or to indicate) the extent  
108 of the hazards, allowing the representation of the spatial distribution of the coastal  
109 hazard. However, it is worth mentioning that the thresholds depend on the hazard  
110 receptor-type (e.g. dunes, salt marsh, houses, infrastructure), defined according to the  
111 Language of Risk (Gouldby and Samuels, 2005) and, therefore, comparisons should be

296  
 297  
 298 112 restricted to similar receptors. These indicators are comparable in concept to the  
 299  
 300 113 Coastal State Indicators (CSI), introduced by van Koningsveld et al (2005). CSI are  
 301  
 302 114 defined as “issue-related parameters that can simply, adequately and quantitatively  
 303 115 describe the dynamic-state and evolutionary trends of a coastal system” (Davidson et  
 304  
 305 116 al., 2006, 2007). The use of process-based indicators can therefore include alongshore  
 306  
 307 117 and cross-shore variability as well as time-dependency (e.g. inclusion of time-scales or  
 308  
 309 118 return periods). The indicators must, however, remain simple on application and  
 310  
 311 119 expression to ensure their applicability by most coastal managers. Examples of  
 312  
 313 120 commonly used process-based indicators (e.g. Wright and Short, 1984 or Masselink  
 314  
 315 121 and Hegge, 1995) include beach morphodynamic state indicators such as the surf  
 316  
 317 122 scaling parameter (Guza and Inman, 1975) and the surf similarity parameter (Battjes,  
 318  
 319 123 1974). However, these are not commonly applied to indicate the degree of coastal hazard.  
 320  
 321 124 In fact, widely accepted process-based indicators to represent storm hazard at sandy  
 322  
 323 125 coasts have not yet been defined and used.



355  
356  
357  
358  
359  
360  
361  
362  
363  
364  
365  
366  
367  
368  
369  
370  
371  
372  
373  
374  
375  
376  
377  
378  
379  
380  
381  
382  
383  
384  
385  
386  
387  
388  
389  
390  
391  
392  
393  
394  
395  
396  
397  
398  
399  
400  
401  
402  
403  
404  
405  
406  
407  
408  
409  
410  
411  
412  
413

127 Figure 1. Scheme representing the steps needed to obtain a process-based indicator,  
128 and its use for hazard assessment. Driving mechanisms and coastal morphology (Step  
129 1) are integrated in numerical models (from simple to complex) to produce a process-  
130 based indicator (step 3) that can be used to express the hazard degree (step 4).  
131 Two possible approaches can be used to obtain the indicator's variability through time:  
132 event approach and response approach (see Divory and McDougal, 2006; Bosom and  
133 Jiménez, 2011; Ferreira et al., 2016). The *event approach*, also called deterministic,  
134 uses the extreme probability distribution of the physical forcing parameter and the  
135 present day coastal morphology (or any simulated condition) to determine the  
136 process-based indicator. The storm parameter (e.g. wave height) for a given return  
137 period is obtained from the corresponding extreme distribution. A formulation/model  
138 (Step 2 on Figure 1) is then applied for the dominant (or other) morphological  
139 condition and the process-based indicator is obtained (e.g. overwash depth, shoreline  
140 retreat) for that return period. In this approach the obtained indicator is then  
141 associated with one value of a storm parameter, for a given return period, losing  
142 significant information on the natural variability of the process (Sánchez-Arcilla et al.,  
143 2009). The *response approach*, also called the probabilistic approach, uses the entire  
144 forcing parameter time-series (e.g. water level, wave height, storm duration) to obtain  
145 the indicators for all known conditions (e.g. runup, erosion) through time. A probability  
146 distribution of extremes must be fitted to the obtained indicator time-series and the  
147 indicator associated with a given return period will be computed from its own  
148 probability distribution. This method is particularly recommended when the forcing  
149 variables are poorly correlated or statistically independent (Bosom and Jiménez, 2011).



414  
415  
416  
417  
418  
419  
420  
421  
422  
423  
424  
425  
426  
427  
428  
429  
430  
431  
432  
433  
434  
435  
436  
437  
438  
439  
440  
441  
442  
443  
444  
445  
446  
447  
448  
449  
450  
451  
452  
453  
454  
455  
456  
457  
458  
459  
460  
461  
462  
463  
464  
465  
466  
467  
468  
469  
470  
471  
472

150  
  
151  
  
152  
153  
154  
155  
156  
157  
158  
159  
160  
161  
162  
163  
164  
  
165  
166  
167  
168  
169  
170  
171  
172

### 3. Proposed process-based indicators

A large number of the indicators that are currently used are frequently poorly defined (Carapuço et al., 2016). The existing lack of standardization of concepts and assumptions restricts the comparability between indicators and among different coastal areas (Nguyen et al., 2016). The use of different indicators may even result in significantly different hazard estimates, requiring greater caution in the selection of the appropriate indicators (Hanslow, 2007). All above expressed shortcomings call for a standardized approach, with clear guidelines for the determination and applicability of hazard indicators. Indicators should, therefore, be as simple as possible, unambiguous, reproducible in different coastal regions, and based on a consistent methodology that enables comparison between sites (see Carapuço et al., 2016; Nguyen et al., 2016). Moreover, they should be suitable for defining the morphodynamic and hydrodynamic state of sedimentary coasts, in support of coastal zone management (Davidson et al., 2006).

The indicators analysed in this paper are process-based and therefore describe the dynamic interaction between the coastal morphological states and the driving mechanisms of the particular hazard. The computation of the proposed indicators for existing (or hindcast) data time-series, and subsequent probabilistic analysis of the indicators' distribution, will allow their use in association with return periods. Since the selected indicators are applicable to sandy coastal areas and can be associated with a given probability of occurrence, they allow direct comparisons or ranking of the hazard intensity between different coastal areas. For each indicator a set of thresholds can be

473  
474  
475  
476  
477  
478  
479  
480  
481  
482  
483  
484  
485  
486  
487  
488  
489  
490  
491  
492  
493  
494  
495  
496  
497  
498  
499  
500  
501  
502  
503  
504  
505  
506  
507  
508  
509  
510  
511  
512  
513  
514  
515  
516  
517  
518  
519  
520  
521  
522  
523  
524  
525  
526  
527  
528  
529  
530  
531

173 established (at local, regional or international level) that can be used to classify and  
174 rank the hazard. Those limits will not be the subject of detailed analysis in this paper,  
175 although application examples will be mentioned after the physical description of each  
176 indicator.

177

178 Overwash indicators

179 Overwash occurs when wave induced runup overtops the foredune ridge or the  
180 highest beach/barrier elevation if the dune is absent. Following Matias and Masselink  
181 (2017) the overwash is a discontinuous flow of seawater and sediment over the  
182 dune/beach crest, which will propagate inland for a given extent (distance to the initial  
183 dune/beach crest position). The two main indicators reflecting overwash induced  
184 hazards are: *overwash potential* and *overwash depth*. Overwash potential is defined as  
185 the vertical difference (in meters) between the potential wave runup (along an  
186 imaginary extended beach/dune slope) and the dune/beach crest elevation (Matias et  
187 al., 2012, 2016; Figure 2). Overwash depth can be defined (adapted from Donnelly,  
188 2008) as the water depth (in meters) at a point (dune crest or backbarrier) during an  
189 overwash event. Overwash depth decreases with the distance across the backbarrier  
190 until reaching a zero value at the maximum inland overwash extent (Figure 2).  
191 Computation of both indicators requires the use of empirical equations to predict the  
192 runup (e.g. Holman, 1986; Stockdon et al., 2006; see Matias et al., 2012 for a review on  
193 formulations) and a digital terrain model. For complex environments, such as partially  
194 engineered coastlines or areas with a complex geomorphological framework, process-  
195 based models should be used to determine such indicators.

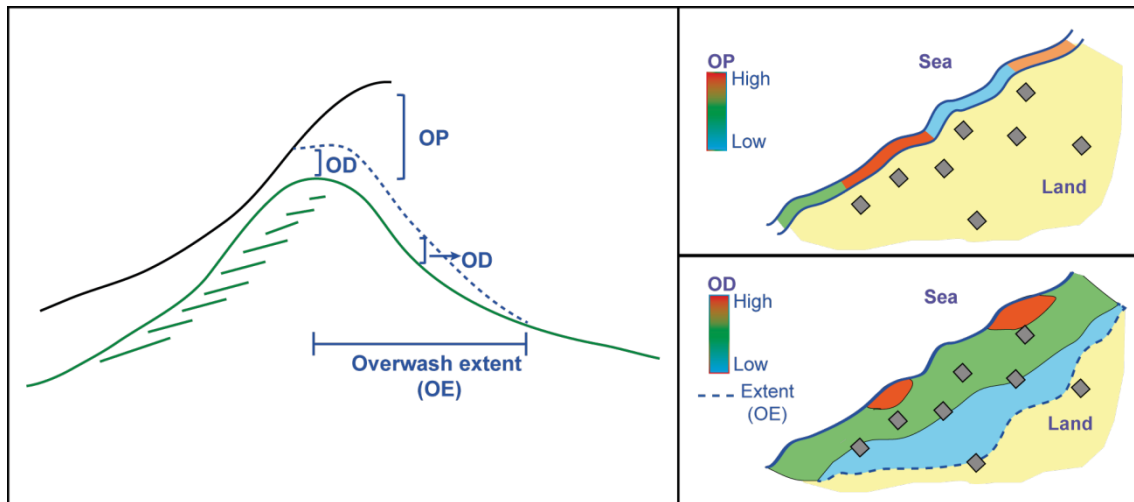
532  
533  
534  
535  
536  
537  
538  
539  
540  
541  
542  
543  
544  
545  
546  
547  
548  
549  
550  
551  
552  
553  
554  
555  
556  
557  
558  
559  
560  
561  
562  
563  
564  
565  
566  
567  
568  
569  
570  
571  
572  
573  
574  
575  
576  
577  
578  
579  
580  
581  
582  
583  
584  
585  
586  
587  
588  
589  
590

196 Both indicators (overwash potential and overwash depth) state a vertical difference  
197 between a water level associated with the overwash and the terrain (Figure 2). The  
198 overwash potential is easier to use because of its computational simplicity since it  
199 compares the result of a runup formulation with the height of the dune/berm crest.  
200 The overwash depth needs extra formulations to determine the effective water lens  
201 depth at the crest and its cross-shore variability (see Donnelly, 2008). However, the  
202 overwash depth has the advantage of being physically representative of the actual  
203 process as it can be applied not only at the dune/beach crest but also at the  
204 backbarrier up to the maximum extent of the overwash (Figure 2). The computation of  
205 the overwash depth can be performed using the formulations proposed in Donnelly  
206 (2008), relating the overwash depth with infiltration and the velocity of the overwash  
207 flux. However, this approach has not been calibrated for all grain-sizes and assumes a  
208 simplified morphology. Overwash depth values at the back of the dune can be  
209 estimated by using an exponential decay that varies according to infiltration and lateral  
210 expansion of the flow. This also allows the definition of a maximum *overwash extent*  
211 which represents the total cross-shore extension of the overwash and can be applied  
212 as an indicator of the area prone to be flooded (e.g. Garcia et al., 2010; Ferreira et al.,  
213 2016; Christie et al., 2017). The inclusion of processes like infiltration and lateral  
214 expansion increases the applicability of the method by providing free parameters that  
215 can be set to local conditions and used as calibration parameters. A more effective  
216 (but also more complex and computationally demanding) way to compute the  
217 overwash depth is to use 1D or 2D numerical models. Other potential indicator to state  
218 the overwash hazard (for expected damages) is the overwash velocity. This is currently  
219 obtained (with limited field validation) by using models and it is therefore of restricted

591  
592  
593  
594  
595  
596  
597  
598  
599  
600  
601  
602  
603  
604  
605  
606  
607  
608  
609  
610  
611  
612  
613  
614  
615  
616  
617  
618  
619  
620  
621  
622  
623  
624  
625  
626  
627  
628  
629  
630  
631  
632  
633  
634  
635  
636  
637  
638  
639  
640  
641  
642  
643  
644  
645  
646  
647  
648  
649

220 application. Alternatively, the overwash velocity can be estimated as a function of the  
221 overwash depth at the dune crest, as determined by Donnelly (2008) and Matias et al.  
222 (2016).

223 Existing studies mostly use the overwash depth and the overwash potential to  
224 determine the possibility of overwash for a given event. Negative values of these  
225 indexes are associated with swash or collision states, according to the storm impact  
226 scale proposed by Sallenger (2000), while positive values imply overwash (e.g. Almeida  
227 et al., 2012; Rodrigues et al., 2012) or higher hazard levels such as inundation (e.g.  
228 Bosom and Jiménez, 2011). Several researchers have applied the overwash potential  
229 indicator in order to find a storm threshold for morphological changes (e.g. Stockdon  
230 et al., 2007; Almeida et al., 2012; Armaroli et al., 2012; Del Río et al., 2012; Haerens et  
231 al., 2012; Trifonova et al., 2012). The use of the overwash depth is still limited (e.g.,  
232 Ferreira et al., 2016; Poelhekke et al., 2016; Valchev et al., 2016; Christie et al., 2017)  
233 since it is not directly obtained by the most commonly used formulas (e.g. Holman,  
234 1986; Stockdon et al., 2006) and has been rarely measured in the field, leading to lack  
235 of validation. However, it has to be stated that overwash depth is a measurable value  
236 in the field in contrast with the overwash potential. For gravel barriers and laboratory  
237 conditions, such measurements have been obtained by Matias et al. (2011) as a result  
238 of the Bardex Project (Williams et al., 2009). Future application of the overwash depth  
239 and overwash potential values should be based on severity scales, to be developed at  
240 local, regional or even international levels, as a function of the potential hazard  
241 associated with each overwash level. Specific depth damage curves can then be  
242 obtained to assess the risk associated with overwash such as already exists for riverine  
243 floods.



244

245 Fig 2. Cross-shore and plan view representing the concept and application of overwash  
 246 indicators. Grey squares represent the location of the hazard receptors (e.g. houses).  
 247 OD - overwash depth; OP - overwash potential; OE - overwash extent.

248

249 Inundation indicators

250 Inundation, which is here defined according to the concept proposed by Sallenger  
 251 (2000), occurs when the storm related still water level (tide + surge) is sufficient to  
 252 completely and continuously submerge a barrier (i.e. the dune crest or the highest  
 253 barrier elevation). Inundation should not be confused with overwash, were an  
 254 intermittent runup level overpasses the barrier for short periods (seconds), and must  
 255 be treated separately as different time (hours to days) and spatial (larger areas and  
 256 depths) scales are involved. Important processes for tide/surge interactions that can  
 257 affect the water level (surge height) are surge propagation during the tidal cycle and  
 258 wind forcing. The continental shelf depth and width are important factors on the  
 259 amplification (mainly for shallow and wide shelves) of both processes (see Fortunato et  
 260 al., 2016). Finally, the storm trajectory and the timing of the storm affect the total

650  
651  
652  
653  
654  
655  
656  
657  
658  
659  
660  
661  
662  
663  
664  
665  
666  
667  
668  
669  
670  
671  
672  
673  
674  
675  
676  
677  
678  
679  
680  
681  
682  
683  
684  
685  
686  
687  
688  
689  
690  
691  
692  
693  
694  
695  
696  
697  
698  
699  
700  
701  
702  
703  
704  
705  
706  
707  
708

709  
710  
711  
712  
713  
714  
715  
716  
717  
718  
719  
720  
721  
722  
723  
724  
725  
726  
727  
728  
729  
730  
731  
732  
733  
734  
735  
736  
737  
738  
739  
740  
741  
742  
743  
744  
745  
746  
747  
748  
749  
750  
751  
752  
753  
754  
755  
756  
757  
758  
759  
760  
761  
762  
763  
764  
765  
766  
767

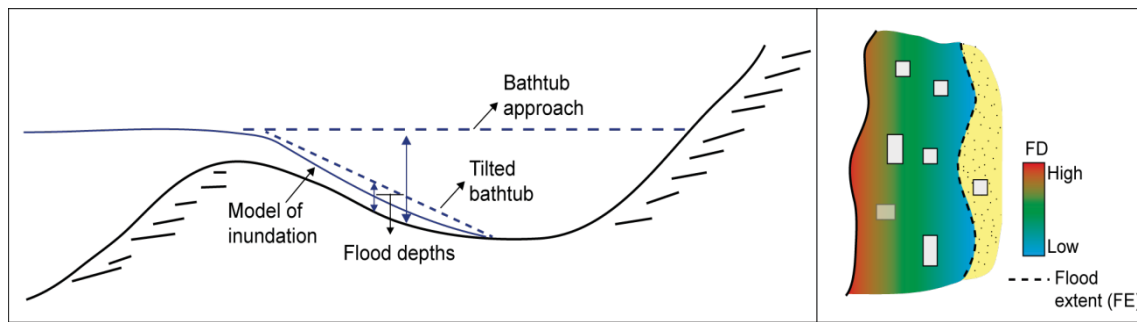
261 water level (Bertin et al., 2012). For small areas, the total water level can be assumed  
262 constant but when the inundation affects very large areas a variable level could be  
263 applied (Breilh, et al., 2014).

264 The extent of the inundation can be determined through several methods with  
265 different degrees of complexity. A simple bathtub model approach can be used for  
266 areas with low morphological complexity (Figure 3). In this method, a given area  
267 becomes inundated if its elevation is less than the water level (Poulter and Halpin,  
268 2008) while a vertical water depth can be computed at each point. The method does  
269 not account for infiltration, roughness or shear stress and therefore it can lead to  
270 overestimation. An adaptation can be performed in order to reduce the level of error  
271 on the estimation of the inundated area and water depth by using a tilted water  
272 surface (Figure 3) along a sloping plane (see Sekovski et al., 2015) based on historical  
273 information and cartography. Problems arise from the application of this simple  
274 methodology when the total inundated area is large and therefore the time needed to  
275 achieve complete inundation is too long when compared with the actual flooding time.  
276 This is particularly valid in inundation areas subjected to tides, where the inundation  
277 level can occur for just a few hours. In such cases, more complex methods, such as the  
278 flood intensity index (Dottori et al., 2016) should be applied. This index reproduces  
279 flooding processes using as theoretical background the 1D uniform flow equation, and  
280 considers the vertical differences between the water level at a given source of the flow  
281 and the elevation of the adjacent terrain. Inundation models, such as LISFLOOD (De  
282 Roo et al., 2000), which can account for lateral connectivity and permeability, can also  
283 be used to better represent the inundation area and depth. The main indicator to be  
284 used on hazard assessment should be the *flood depth* (see Figure 3) at each hinterland

768  
769  
770  
771  
772  
773  
774  
775  
776  
777  
778  
779  
780  
781  
782  
783  
784  
785  
786  
787  
788  
789  
790  
791  
792  
793  
794  
795  
796  
797  
798  
799  
800  
801  
802  
803  
804  
805  
806  
807  
808  
809  
810  
811  
812  
813  
814  
815  
816  
817  
818  
819  
820  
821  
822  
823  
824  
825  
826

285 position, which expresses the intensity of the hazard and its variability along each  
286 considered coastal region. Other useful indicators worth of mentioning are the *total*  
287 *flood extent* (see Figure 3) from a given reference point (e.g. the shoreline), and the  
288 *percentage of flooded area per coastal sector* (from the shoreline to a given previously  
289 defined hinterland limit). The *overflowing discharge volume* can also be used. This  
290 indicator is a function of the overflow depth at the crest of a dune or dyke multiplied  
291 by its length and integrated over time using the rectangular weir discharge equation of  
292 Kindsvater and Carter (1957). The extension of the overflowing discharge volume can  
293 be calculated by a step by step increase in the water level until the total volume is  
294 reached. Similarly, the volume can be used in combination with the tilting bathtub  
295 method to compare inundation volumes.

296 An example of the application of the tilted bathtub method can be found in Sekovski et  
297 al. (2015). The authors used both the flood depth (total water level at a given point)  
298 and the flood extent to evaluate present-day and future flood hazards at coastal cities  
299 from Emilia-Romagna (Italy). An inter comparison of the above methods to assess the  
300 inundation caused by the Xynthia storm to La Faute-sur-Mer is provided by Breilh et al.  
301 (2013) and Vousdoukas et al. (2016). Furthermore, Vousdoukas et al. (2016) applied  
302 the above indicators to assess the flood hazard along the entire European coast.  
303 Poulter and Halpin (2008) used and improved the bathtub method by incorporating  
304 the hydrological connectivity between grid cells by considering that only cells that have  
305 a connection with the open sea or with nearby cells are considered flood-prone. Perini  
306 et al. (2016) used the tilted bathtub approach and the Cost Distance tool of ArcGIS to  
307 produce a least-path cost analysis and to remove isolated areas without hydrological  
308 connectivity in order to improve the final flood maps.



309

310 Fig 3. Cross-shore and plan view representing the concept and application of the  
 311 inundation indicators. White polygons represent the location of the hazard receptors  
 312 (e.g. houses, hotels). FD – Flood depth; FE – Flood extent.

313

314 Erosion indicators

315 Erosion in this paper simply refers to short-term (episodic) effects driven by storm  
 316 events or storm groups effecting coastal areas, excluding continuous erosion caused by  
 317 persistence of sediment scarcity. Storm-induced erosion can be observed as a vertical  
 318 lowering of the beach/dune system (or by scarp or bluff formation, including  
 319 subsequent dune avalanching) or as a horizontal inland displacement of the coast (e.g.  
 320 barrier rollover). The erosion associated with storms will not necessarily result on an  
 321 overall and definitive displacement of the shoreline since the coast can recover to its  
 322 original configuration if there is enough sediment available. However, the promoted  
 323 vertical and horizontal shifts are capable of producing destruction and damages if  
 324 occupation or other receptors are present. Three main indicators can be proposed:  
 325 *shoreline/berm retreat, dune foot retreat, and vertical erosion* (all in meters) at a given  
 326 point (e.g. dune foot, dune crest, at the infrastructure) (Figure 4). The shoreline/berm  
 327 retreat and the dune foot retreat represent the horizontal displacement produced by

827  
828  
829  
830  
831  
832  
833  
834  
835  
836  
837  
838  
839  
840  
841  
842  
843  
844  
845  
846  
847  
848  
849  
850  
851  
852  
853  
854  
855  
856  
857  
858  
859  
860  
861  
862  
863  
864  
865  
866  
867  
868  
869  
870  
871  
872  
873  
874  
875  
876  
877  
878  
879  
880  
881  
882  
883  
884  
885



886  
887  
888  
889  
890  
891  
892  
893  
894  
895  
896  
897  
898  
899  
900  
901  
902  
903  
904  
905  
906  
907  
908  
909  
910  
911  
912  
913  
914  
915  
916  
917  
918  
919  
920  
921  
922  
923  
924  
925  
926  
927  
928  
929  
930  
931  
932  
933  
934  
935  
936  
937  
938  
939  
940  
941  
942  
943  
944

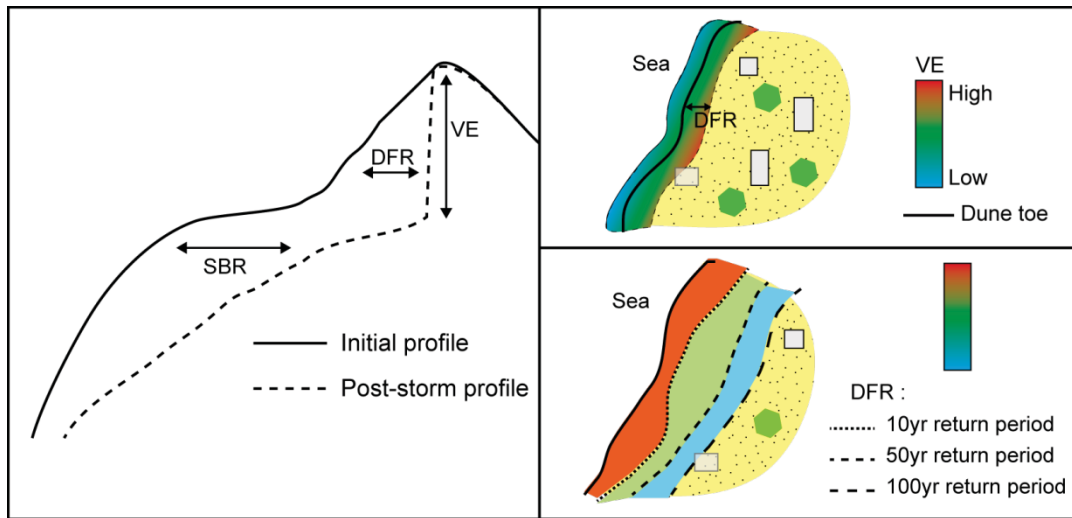
328 the storm at a given coastal feature (Figure 4), and can be directly compared with  
329 occupation to assess vulnerability. The use of the shoreline/berm retreat versus the  
330 dune foot retreat as indicators depends very much on the exposed elements to be  
331 assessed. For coastal areas with infrastructure located on the beach berm or on the  
332 beach face (e.g. bars, amenities) the shoreline/berm retreat should be used, which can  
333 then be transformed (or not) into a remaining beach width or into a distance to  
334 occupation. For coastal areas where development and infrastructure (e.g. houses,  
335 roads) are located on the dune or at the hinterland, the dune foot retreat should be  
336 applied. This can also be transformed into a remaining distance to the developed area  
337 when necessary/applicable. The use of the shoreline/berm retreat versus the dune  
338 foot retreat also depends on the coastal morphology; at sandy coasts without a dune  
339 the shoreline/berm retreat should be used. The vertical erosion corresponds to the  
340 vertical difference between the original morphology and the computed/observed  
341 morphology during and after the storm (Figure 4). Vertical differences can result in  
342 potential damage for the existing development on the beach. This indicator can be  
343 equally used on the berm, dune or backbarrier, for any storm and given morphological  
344 characteristics, allowing the cross-shore determination and comparison of the vertical  
345 erosion indicator. The retreat/erosion indicators can be computed by using relatively  
346 simple analytical models, such as the convolution model (Kriebel and Dean, 1993),  
347 Larson's method (Larson et al., 2004), the erosion structural function (Mendoza and  
348 Jiménez, 2006), or the ShoreFor behaviour model (Davidson et al., 2013), among many  
349 others. These models use relatively simple analytical formulations that integrate  
350 driving mechanisms (such as wave height, storm duration and sea level) jointly with  
351 the morphological and sedimentological characteristics of the coastal area (e.g. dune

945  
946  
947  
948  
949  
950  
951  
952  
953  
954  
955  
956  
957  
958  
959  
960  
961  
962  
963  
964  
965  
966  
967  
968  
969  
970  
971  
972  
973  
974  
975  
976  
977  
978  
979  
980  
981  
982  
983  
984  
985  
986  
987  
988  
989  
990  
991  
992  
993  
994  
995  
996  
997  
998  
999  
1000  
1001  
1002  
1003

352 height, berm width, beach slope or grain size) to determine coastal erosion (volume or  
353 retreat) induced by each storm. All the above methods deal with swash and collision  
354 conditions but not with overwash and inundation. For the later regimes, the erosion  
355 processes are different and generally more complex. Process-based models, like  
356 XBeach (Roelvink et al., 2009), can also be employed to determine the same indicators,  
357 for all regimes and with greater detail but requiring a higher level of computational  
358 complexity and available data for model calibration. Process-based models like XBeach  
359 reproduce the processes occurring at coastal areas during a storm, containing the  
360 essential physics of dune erosion, overwash, avalanching, swash, infragravity waves  
361 and wave groups (Roelvink et al., 2009). Finally, if LIDAR (Light Detection and Ranging)  
362 or similar resolution/quality data (e.g. from UAVs or satellite imagery) exists for pre-  
363 and post-storm conditions the erosion indicators can also be computed based on  
364 direct measurements (for example by comparing pre and post storm digital terrain  
365 models) and for all storm impact regimes following the method of Stockdon et al.  
366 (2007).

367 According to Ciavola et al. (2015) dune erosion volume, berm retreat or dune height  
368 reduction can be used directly or against thresholds to identify areas prone or resistant  
369 to erosion hazards. Nevertheless, the use of process-based erosion indicators is not  
370 widespread, with trend indicators such as shoreline position, high water line,  
371 vegetation line or scarp location (see Hanslow, 2007) being the most widely used. The  
372 sub-aerial beach and dune volume are also used as coastal indicators (Hanslow, 2007;  
373 Armaroli et al., 2012) but not necessarily as process-based indicators, with exceptions  
374 such as the use of the erosion resistance index by Judge et al. (2003), the eroded  
375 volume and the beach retreat (e.g. Mendoza and Jiménez, 2006), and the dune

1004  
 1005  
 1006 376 stability factor by Armaroli et al. (2012). Examples of use of process-based erosion  
 1007  
 1008 377 indicators also include the distance between the dune and the shoreline or the  
 1009  
 1010 378 comparison between the momentary coastline position and a given landward  
 1011  
 1012 379 boundary, such as the dune foot (see Davidson et al., 2006).



1016  
 1017  
 1018  
 1019  
 1020  
 1021  
 1022  
 1023  
 1024  
 1025  
 1026  
 1027  
 1028  
 1029  
 1030 380  
 1031  
 1032  
 1033 381 Fig 4. Cross-shore and plan view representing the concept and application of the  
 1034  
 1035 382 erosion indicators. White polygons represent the location of the hazard receptors (e.g.  
 1036  
 1037 383 houses, hotels). SBR – Shoreline/Berm retreat; DFR – Dune foot retreat; VE – Vertical  
 1038  
 1039 384 erosion.

1041  
 1042 385  
 1043  
 1044  
 1045 386 4. Summary of indicators and discussion of use

1046  
 1047  
 1048 387 A synthesis of the reviewed and proposed indicators for three main analysed hazards  
 1049  
 1050 388 (overwash, inundation and erosion), on sandy shores, can be found in Table I. The  
 1051  
 1052 389 proposed process-based indicators are all simple in concept and refer to a measurable  
 1053  
 1054 390 distance, permitting a cartographic expression of the hazard (see figures 2 to 4).  
 1055  
 1056 391 Several indicators report a vertical difference to the initial topographic surface  
 1057  
 1058  
 1059  
 1060  
 1061  
 1062

1063  
1064  
1065 392 (overwash depth, overwash potential, flood depth, vertical erosion) representative of  
1066  
1067 393 an interaction between driving processes (e.g. water level, runup) and such surface (as  
1068  
1069 394 is the case for overwash depth, overwash potential and flood depth) or the result of  
1070  
1071 395 the morphodynamic process measured as a difference between pre and post-event  
1072  
1073 396 surfaces (vertical erosion). Others (overwash extent, flood extent, shoreline/berm  
1074  
1075 397 retreat, and dune foot retreat) register the cross-shore extent of the hazard. The  
1076  
1077 398 alongshore integration of both (vertical and horizontal indicators) allows, in most  
1078  
1079 399 cases, for an overall three-dimensional cartography of the hazard, including the  
1080  
1081 400 potentially affected areas and the vertical level of action. That is, for instance, the case  
1082  
1083 401 of the joint use of the overwash/flood depth and the associated extent. The vertical  
1084  
1085 402 erosion indicator, since it is immediately associated with an inland position, allows a  
1086  
1087 403 direct three-dimensional representation of the hazard when expressed alongshore.  
1088  
1089  
1090 404 The here-reviewed and proposed indicators can be applied on natural sandy (or  
1091  
1092 405 gravely) beaches with or without dune systems or backbarriers. Although the  
1093  
1094 406 indicators are not necessarily limited in their use, some of the proposed approaches  
1095  
1096 407 are, and they can only be applied to coastal areas with low morphological complexity.  
1097  
1098 408 This includes the case of the determination of the flood depth/extent by using a  
1099  
1100 409 bathtub (or tilted bathtub) approach. Most of the existing formulations and models are  
1101  
1102 410 also not completely adapted to heavily developed hinterlands (e.g. dominated by  
1103  
1104 411 impermeable surfaces) and will require some adaptation. Previous knowledge of the  
1105  
1106 412 dominant processes during storms will also help to correctly select the methods and  
1107  
1108 413 indicators to use in the most cost-effective way.  
1109  
1110  
1111  
1112  
1113  
1114  
1115  
1116  
1117  
1118  
1119  
1120  
1121

1122  
1123  
1124  
1125  
1126  
1127  
1128  
1129  
1130  
1131  
1132  
1133  
1134  
1135  
1136  
1137  
1138  
1139  
1140  
1141  
1142  
1143  
1144  
1145  
1146  
1147  
1148  
1149  
1150  
1151  
1152  
1153  
1154  
1155  
1156  
1157  
1158  
1159  
1160  
1161  
1162  
1163  
1164  
1165  
1166  
1167  
1168  
1169  
1170  
1171  
1172  
1173  
1174  
1175  
1176  
1177  
1178  
1179  
1180

414 A direct comparison on the applicability of selected (based on the works of Carapuço  
415 et al., 2016 and Nguyen et al., 2016) geo- and driver- based indicators against the  
416 proposed process-based indicators is expressed at Table II. Most geo- and driver-based  
417 indicators are easier to obtain since they can be directly extracted from existing  
418 cartography or field measurements (geoindicators) and from instrumental  
419 measurements or hindcast predictions (driver-based indicators) often available on-line.  
420 They are commonly converted into several simple semi-quantitative values (e.g. from 1  
421 to 5) that are added (quantified) alongshore to permit a representation of the hazard,  
422 making them simple to use even for non-experts. They are therefore still used as a  
423 simple methodology to classify the coast according to its vulnerability (e.g. Jiménez et  
424 al., 2016). They do not, however, account for the acting processes and can therefore  
425 affect the final results as observed by Judge et al. (2003) when considering the crest  
426 height as a predictor of dune vulnerability. Process-based indicators require both geo-  
427 and driver-based information and the additional use of formulations/models, to obtain  
428 a final value. If using return periods, a statistical analysis (for either the event or  
429 response approach) is also required. This implies, from the users, a higher expertise on  
430 coastal dynamics, including the perception of the physical processes acting in coastal  
431 areas and responsible for hazards. This reduces the applicability of process-based  
432 indicators to users with sufficient background on coastal dynamics. Process-based  
433 indicators have, however, several advantages that will, most probably, increase their  
434 future use. Most indicators have the possibility of including both detailed longshore  
435 variability and cross-shore expression of the hazard, while driver-based indicators have  
436 a reduced representativeness of the longshore variability, mainly if wave propagation  
437 models are not used. Most used geo and driver-based indicators are also not able to

1181  
1182  
1183 438 include the cross-shore expression of the hazard (with the exception of the erosion  
1184  
1185 439 rate).  
1186  
1187  
1188 440 Geo- and driver-based indicators when used alone are often site-specific and hardly  
1189  
1190 441 comparable between coastal areas. Process-based indicators present an outcome that  
1191  
1192 442 can be easily compared among sites. For instance, the vertical expression of a hazard  
1193  
1194 443 (e.g. flood depth or overwash depth) can be compared between coastal regions with  
1195  
1196 444 similar settings and a higher value of the indicator will represent a potentially higher  
1197  
1198 445 hazard. That is not the case for driver-based indicators, for instance. A higher wave  
1199  
1200 446 height or water level cannot be compared between coastal areas since the hazard will  
1201  
1202 447 depend on the relationship with the coastal elevation. A lower value of a driver-based  
1203  
1204 448 indicator can be responsible for a higher hazard if the coastal elevation is low, and the  
1205  
1206 449 opposite is also valid. This prevents the compared use of geo- and driver-based  
1207  
1208 450 indicators to assess the hazard for distinct coastal areas. The extensive use of process-  
1209  
1210 451 based indicators, for different coastal regions will allow, in the future, the  
1211  
1212 452 development of hazard levels/scales that can be internationally adopted. Since  
1213  
1214 453 process-based indicators can be associated with a given probability of occurrence and  
1215  
1216 454 can be directly compared between coastal regions, they can also be used to rank the  
1217  
1218 455 hazard intensity for vast coastal areas, for equal return periods. It must however be  
1219  
1220 456 stressed that, for the moment, no universal application of indicators exists and that  
1221  
1222 457 there are no internationally widely accepted intervals to classify each indicator  
1223  
1224 458 according to the potential hazard. This is still work to be performed, to be based on the  
1225  
1226 459 lessons learned from the application of process-based indicators at a large-scale.  
1227  
1228  
1229  
1230  
1231  
1232  
1233  
1234  
1235  
1236  
1237  
1238  
1239

1240  
1241  
1242 460 The here proposed process-based indicators do not integrate feedback mechanisms  
1243  
1244 461 resulting from the interaction between morphology and forcing agents (e.g. waves,  
1245  
1246 462 currents). That is also the case for goindicators and for indicators solely based on  
1247  
1248 463 driving mechanisms. The hazard and consequent risk can change as a result of  
1249  
1250 464 feedback mechanisms. For instance, the lowering of a dune by overwash will increase  
1251  
1252 465 the overwash potential and the overwash depth, leading to an increase in the hazard  
1253  
1254 466 when compared with the initial (and considered) situation/morphology. The feedback  
1255  
1256 467 mechanism can occur differently alongshore, as a function of the nearshore, shoreface  
1257  
1258 468 and dune morphologies. In cases where feedback mechanisms may be highly relevant,  
1259  
1260 469 these (and other indexes) may not fully reflect the impacts associated with a given  
1261  
1262 470 event. In those cases only process-based models with high resolution topo-  
1263  
1264 471 bathymetric grids, after validation and calibration, may be helpful to better understand  
1265  
1266 472 the hazard in coastal areas. It must be also kept in mind that the indicators must  
1267  
1268 473 remain simple in concept and application to ensure their use by most coastal  
1269  
1270 474 managers. Highly complex indicators requiring extreme computational effort and a  
1271  
1272 475 high degree of specialization will probably fail to be widely applied by most coastal  
1273  
1274 476 end-users, including managers.

1275  
1276  
1277  
1278  
1279  
1280  
1281 477

## 1282 1283 1284 478 5. Conclusions, limitations and future improvements

1285  
1286  
1287 479 The current use of process-based indicators is still on its infancy, being necessary to  
1288  
1289 480 establish a set of the most relevant indicators that can better express potential hazards  
1290  
1291 481 at sandy (and gravelly) shores:

- 1292  
1293  
1294  
1295 482 • Overwash: overwash depth, potential and extent;

- 1299  
1300  
1301 483       • Inundation: flood depth and extent;  
1302  
1303  
1304 484       • Erosion: shoreline/berm and dune foot retreat, and vertical erosion.  
1305

1306  
1307 485       The future use of process-based indicators to quantify coastal hazards is  
1308  
1309 486       recommended, mainly when compared to the most classical and commonly used geo-  
1310  
1311 487       and driver-based indicators, since they allow:

- 1312  
1313  
1314 488       a) better quantification of the hazard by representing the interaction between  
1315  
1316 489       forcing mechanisms and morphology;  
1317  
1318  
1319 490       b) better expression of the alongshore and cross-shore (extent) variability of the  
1320  
1321 491       hazard, including its three-dimensional representation (longshore, cross-shore  
1322  
1323 492       and vertical); and  
1324  
1325 493       c) comparison between coastal areas.  
1326  
1327

1328  
1329 494       The development of the process-based indicators' potential will rely on their  
1330  
1331 495       generalised use in the future. Only an increase in their use will allow the definition of  
1332  
1333 496       common hazard levels for distinct coastal regions and a large-scale application to vast  
1334  
1335 497       areas (e.g. at pan-European level). A few limitations still exist that prevent the wider  
1336  
1337 498       use of these indicators. These include:

- 1338  
1339  
1340 499       i)       limited available quality data for several regions, regarding either  
1341  
1342 500       morphologic and hydrodynamic parameters, which is particularly relevant  
1343  
1344 501       when long-term time-series (e.g. wave characteristics) are needed to better  
1345  
1346 502       define return periods;  
1347  
1348  
1349 503       ii)      restricted current use of formulations and models by end-users and namely  
1350  
1351 504       coastal managers;  
1352  
1353  
1354  
1355  
1356  
1357



1358  
1359  
1360  
1361  
1362  
1363  
1364  
1365  
1366  
1367  
1368  
1369  
1370  
1371  
1372  
1373  
1374  
1375  
1376  
1377  
1378  
1379  
1380  
1381  
1382  
1383  
1384  
1385  
1386  
1387  
1388  
1389  
1390  
1391  
1392  
1393  
1394  
1395  
1396  
1397  
1398  
1399  
1400  
1401  
1402  
1403  
1404  
1405  
1406  
1407  
1408  
1409  
1410  
1411  
1412  
1413  
1414  
1415  
1416

505       iii)     reduced possibility of integrating feedback mechanisms, with the exception  
506                   of the most complex process-based models.

507     The first limitation will be solved (with time) by the ongoing and increasing  
508     improvement on data access (and quality) worldwide, including on-line access to  
509     coastal morphology and wave/water level series. To obviate the second limitation an  
510     improvement will be needed on the transfer of knowledge from the coastal scientific  
511     community towards coastal end-users. The third limitation will be solved by integrating  
512     process-based models into user-friendly frameworks for generalised use. The  
513     improved and generalised use of process-based indicators will provide coastal  
514     managers with a highly relevant tool to evaluate coastal hazards and risks and,  
515     therefore, to better establish and implement disaster risk reduction in the future, in  
516     the most cost-effective way.

517

518                   Acknowledgments

519     This work was supported by the European Community's 7th Framework Programme  
520     through the grant to RISC-KIT ("Resilience-increasing Strategies for Coasts - Toolkit"),  
521     contract no. 603458, and by contributions by the partner institutes. Susana Costas  
522     research is funded through the "FCT Investigator" program (ref. IF/01047/2014). This  
523     work was also supported by the Portuguese Science Foundation (FCT) through the  
524     grant UID/MAR/00350/2013 attributed to CIMA/University of Algarve

525

526                   References

1417  
1418  
1419 527 Almeida, L.P., Ferreira, O., Taborda, R., 2011. Geoprocessing tool to model beach  
1420  
1421 528 erosion due to storms: application to Faro beach (Portugal). *Journal of Coastal*  
1422  
1423 *Research*, SI 64, 1830-1834.  
1424 529  
1425  
1426  
1427 530 Almeida L. P., Vousedoukas M. V., Ferreira O., Rodrigues, B.A., Matias, A., 2012.  
1428  
1429 531 Thresholds for storm impacts on an exposed sandy coastal area in southern Portugal,  
1430  
1431 532 *Geomorphology*, 143, 3-12. DOI: 10.1016/j.geomorph.2011.04.047  
1432  
1433  
1434 533 Armaroli, C., Ciavola, P., Perini, L., Calabrese, L., Lorito, S., Valentini, A., Masina, M.,  
1435  
1436 534 2012. Critical storm thresholds for significant morphological changes and damage  
1437  
1438 535 along the Emilia-Romagna coastline, Italy. *Geomorphology*, 143, 34-51.  
1439  
1440 536 DOI: 10.1016/j.geomorph.2011.09.006  
1441  
1442  
1443  
1444 537 Battjes, J.A., 1974. Surf similarity. *Coastal Engineering*'74, 446-480.  
1445  
1446  
1447 538 Bennington, B. and Farmer, E.C., 2015. *Learning from the impacts of Superstorm Sandy*.  
1448  
1449 539 Ed. J. Bret Bennington and E.Christa Farmer. Academic Press. Elsevier, 123 p.  
1450  
1451  
1452 540 Bertin, X., Bruneau, N., Breilh, J.F., Fortunato, A.B., Karpytchev, M., 2012. Importance  
1453  
1454 541 of wave age and resonance in storm surges: The case Xynthia, Bay of Biscay. *Ocean*  
1455  
1456 542 *Modelling*, 42, 16-30. DOI: 10.1016/j.ocemod.2011.11.001  
1457  
1458  
1459  
1460 543 Bosom, E. and Jiménez, J.A., 2011. Probabilistic coastal vulnerability assessment to  
1461  
1462 544 storms at regional scale - application to Catalan beaches (NW Mediterranean). *Natural*  
1463  
1464 545 *Hazards and Earth System Sciences*, 11, 475-484. DOI: 10.5194/nhess-11-475-2011  
1465  
1466  
1467 546 Breilh, J.F., Chaumillon, E., Bertin, X., Gravelle, M., 2013. Assessment of static flood  
1468  
1469 547 modeling techniques: application to contrasting marshes flooded during Xynthia  
1470  
1471  
1472  
1473  
1474  
1475

1476  
1477  
1478 548 (western France). *Natural Hazards Earth Systems Science*, 13, 1595-1612.  
1479  
1480 549 DOI:10.5194/nhess-13-1595-2013  
1481  
1482  
1483 550 Bush, D.M., Neal, W.J., Young, R.S., Pilkey, O.H., 1999. Utilization of geoinicators for  
1484  
1485 551 rapid assessment of coastal-hazard risk and mitigation. *Ocean and Coastal*  
1486  
1487 552 *Management*, 42, 647-670. DOI: 10.1016/S0964-5691(99)00027-7  
1488  
1489  
1490  
1491 553 Callaghan , D.P., Nielsen, P., Short, A., Ranasinghe, R., 2008. Statistical simulation of  
1492  
1493 554 wave climate and extreme beach erosion. *Coastal Engineering*, 55(5), 375-390.  
1494  
1495 555 DOI:10.1016/j.coastaleng.2007.12.003  
1496  
1497  
1498 556 Carapuço, M.M., Taborda, R., Silveira, T.M., Psuty, N.P., Andrade, C., Freitas, M.C.,  
1499  
1500 557 2016. Coastal geoinicators: Towards the establishment of a common framework for  
1501  
1502 558 sandy coastal environments. *Earth-Science Reviews*, 154, 183-190. DOI:  
1503  
1504 559 10.1016/j.earscirev.2016.01.002  
1505  
1506  
1507  
1508 560 Castelle, B., Marieu, V., Bujan, S., Splinter, K.D., Robinet, A., Senechal, N., Ferreira, S.,  
1509  
1510 561 2015. Impact of the winter 2013-2014 series of severe Western Europe storms on a  
1511  
1512 562 double-barred sandy coast: Beach and dune erosion and megacusp embayments.  
1513  
1514 563 *Geomorphology*, 238, 135-148. DOI: 10.1016/j.geomorph.2015.03.006  
1515  
1516  
1517  
1518 564 Christie, E.K., Spencer, T., Owen, D., McIvor, A.L., Möller, I., Viavattene, C., 2017.  
1519  
1520 565 Regional coastal flood risk assessment for a tidally dominant, natural coastal setting:  
1521  
1522 566 North Norfolk, southern North Sea. *Coastal Engineering*, in press. DOI:  
1523  
1524 567 10.1016/j.coastaleng.2017.05.003  
1525  
1526  
1527  
1528  
1529  
1530  
1531  
1532  
1533  
1534

1535  
1536  
1537 568 Ciavola, P., Ferreira, O., van Dongeren, A., de Vries, J., Armaroli, C., Harley, M., 2015.  
1538  
1539 569 Prediction of storms impacts on beach and dune systems. In: *Hydrometeorological*  
1540  
1541 570 *Hazards: Interfacing Science and Policy*. Ed: Philippe Quevauviller, John Wiley & Sons.  
1542  
1543  
1544  
1545 571 Clay, P.M., Colburn, L.L., Seara, T., 2016. Social bonds and recovery: An analysis of  
1546  
1547 572 Hurricane Sandy in the first year after landfall. *Marine Policy*, 74, 334-340. DOI:  
1548  
1549 573 10.1016/j.marpol.2016.04.049  
1550  
1551  
1552 574 Davidson, M.A., Aarninkhof, S., van Koningsveld, M., Holman, R.A., 2006. Developing  
1553  
1554 575 coastal video monitoring systems in support of coastal zone management. *Journal of*  
1555  
1556 576 *Coastal Research*, SI 39, 49-56.  
1557  
1558  
1559  
1560 577 Davidson, M.A., van Koningsveld, M., de Kruif, A., Rawson, J., Holman, R., Lamberti, A.,  
1561  
1562 578 Medina, R., Kroon, A., Aarninkhof, S., 2007. The CoastView project: Developing video-  
1563  
1564 579 derived Coastal State Indicators in support of coastal zone management. *Coastal*  
1565  
1566 580 *Engineering*, 54, 463-475. DOI: 10.1016/j.coastaleng.2007.01.007  
1567  
1568  
1569  
1570 581 Davidson, M.A., Splinter, K.D., Turner, I.L., 2013. A simple equilibrium model for  
1571  
1572 582 predicting shoreline change. *Coastal Engineering*, 73, 191-202. DOI:  
1573  
1574 583 10.1016/j.coastaleng.2012.11.002  
1575  
1576  
1577 584 De Roo, A.P.J., Wesseling, C.G., van Deursen, W.P.A., 2000. Physically base driver basin  
1578  
1579 585 modelling within a GIS: the LISFLOOD model. *Hydrological Processes*, 14, 1981-1992.  
1580  
1581 586 DOI: 10.1002/1099-1085(20000815/30)14:11/12<1981::AID-HYP49>3.0.CO;2-F  
1582  
1583  
1584  
1585 587 Del Río, L., Plomaritis, T.A., Benavente, J., Valladares, M., Ribera, P., 2012. Thresholds  
1586  
1587 588 for storm impacts along European coastlines. *Geomorphology*, 143-144, 13-23.  
1588  
1589 589 DOI:10.1016/j.geomorph.2011.04.048  
1590  
1591  
1592  
1593

1594  
1595  
1596 590 Divory, D. and McDougal, W.G., 2006. Response-based coastal flood analysis.  
1597  
1598 591 *Proceedings of the 30<sup>th</sup> International Conference on Coastal Engineering*, 5291-5301,  
1599  
1600 ASCE.  
1601  
1602  
1603  
1604 593 Donnelly, C., 2008. *Coastal Overwash: Processes and Modelling*. PhD Thesis. Lund  
1605  
1606 594 University, Sweden, 53 pp.  
1607  
1608  
1609 595 Dottori, F., Martina, M.L.V., Figueiredo, R., 2016. A methodology for flood  
1610  
1611 596 susceptibility and vulnerability analysis in complex flood scenarios. *Journal of Flood*  
1612  
1613 *Risk Management*, DOI: 10.1111/jfr3.12234  
1614  
1615  
1616 598 Durán, R., Guillén, J., Ruiz, A., Jiménez, J.A., Sagristà, E., 2016. Morphological changes,  
1617  
1618 599 beach inundation and overwash caused by an extreme storm on a low-lying embayed  
1619  
1620 beach bounded by a dune system (NW Mediterranean). *Geomorphology*, 274, 129-142.  
1621  
1622 DOI: 10.1016/j.geomorph.2016.09.012  
1623  
1624  
1625  
1626 602 Ferreira, O., Viavattene, C., Jiménez, J., Bole, A., Plomaritis, T., Costas, S., Smets, S.,  
1627  
1628 603 2016. CRAF Phase 1, a framework to identify coastal hotspots to storm impacts. *E3S*  
1629  
1630 *Web Conf.* 7, 11008 (FLOODrisk 2016: 3rd European Conference on Flood Risk  
1631  
1632 Management).  
1633  
1634  
1635  
1636 606 Fortunato, A.B., Li, K., Bertin, X., Rodrigues, M., Miguez, B.M., 2016. Determination of  
1637  
1638 607 extreme sea levels along the Iberian Atlantic coast. *Ocean Engineering*, 111, 471-482.  
1639  
1640 DOI:10.1016/j.oceaneng.2015.11.031  
1641  
1642  
1643  
1644 609 Garcia, T., Ferreira, O., Matias, A., Dias, J.A., 2010. Overwash vulnerability assessment  
1645  
1646 610 based on long-term washover evolution. *Natural Hazards*, 54, 225-244. DOI:  
1647  
1648 611 10.1007/s11069-009-9463-3  
1649  
1650  
1651  
1652

1653  
1654  
1655  
1656  
1657  
1658  
1659  
1660  
1661  
1662  
1663  
1664  
1665  
1666  
1667  
1668  
1669  
1670  
1671  
1672  
1673  
1674  
1675  
1676  
1677  
1678  
1679  
1680  
1681  
1682  
1683  
1684  
1685  
1686  
1687  
1688  
1689  
1690  
1691  
1692  
1693  
1694  
1695  
1696  
1697  
1698  
1699  
1700  
1701  
1702  
1703  
1704  
1705  
1706  
1707  
1708  
1709  
1710  
1711

612 Gouldy, B. and Samuels., P, 2005. Language of Risk – Project Definitions. Report: T32-  
613 04-01.Floodsite Project. Available at [www.floodsite.net](http://www.floodsite.net)

614 Guza, R.T and Inman, D.I., 1975. Edge waves and beach cusps. *Journal of Geophysical*  
615 *Research*, 80, 1328-1342. DOI: 10.1029/JC080i021p02997

616 Haerens, P., Bolle, A., Trouw, K., Houthuys, R., 2012. Definition of storm thresholds for  
617 significant morphological change of the sandy beaches along the Belgian coastline.  
618 *Geomorphology*, 143-144, 104-117. DOI:10.1016/j.geomorph.2011.09.015

619 Hanslow, D.J., 2007. Beach erosion trend measurement: A comparison of trend  
620 indicators. *Journal of Coastal Research*, SI 50, 588-593.

621 Hinkel, J., Lincke, D., Vafeidis, A.T., Perrette, M., Nicholls, R.J., Tol, R.S.J., Marzeion, B.,  
622 Fettweis, X., Ionescu, C., Levermann, A., 2014. Coastal flood damage and adaptation  
623 costs under 21st century sea-level rise, *Proceedings of the National Academy of*  
624 *Sciences of the United States of America*, 111, 3292–3297. doi:  
625 10.1073/pnas.1222469111

626 Holman, R.A., 1986. Extreme value statistics for wave run-up on a natural beach.  
627 *Coastal Engineering*, 9, 527–544. DOI: 10.1016/0378-3839(86)90002-5

628 Jiménez, A.C., Ávila, J.I.E, Lacouture, M.M.V., Casarín, R., 2016. Classification of beach  
629 erosion vulnerability on the Yucatan Coast. *Coastal Management*, 44, 333-349. DOI:  
630 10.1080/08920753.2016.1155038

631 Judge, E.K., Overton, M.F., Fisher, J.S., 2003. Vulnerability indicators for coastal dunes.  
632 *Journal of Waterway, Port, Coastal and Ocean Engineering*, 129, 270-278. DOI:  
633 10.1061/(ASCE)0733-950X(2003)129:6(270)

1712  
1713  
1714 634 Kantha, L., 2013. Classification of hurricanes: Lessons from Katrina, Ike, Irene, Isaac and  
1715  
1716 635 Sandy. *Ocean Engineering*, 70, 124-128. DOI: 10.1016/j.oceaneng.2013.06.007  
1717  
1718  
1719 636 Kindsvater, C. and Carter, R., 1957. Discharge characteristics of rectangular thin-plate  
1720  
1721 637 weirs, *Journal of the Hydraulics Division*, ASCE, 83, 1453/1-1453/36.  
1722  
1723  
1724  
1725 638 Kriebel, D. and Dean, R.G., 1993. Convolution model for time-dependent beach-profile  
1726  
1727 639 response. *Journal of Waterway, Port, Coastal and Ocean Engineering*, 119, 204-226.  
1728  
1729 640 DOI: 10.1061/(ASCE)0733-950X(1993)119:2(204)  
1730  
1731  
1732 641 Larson, M., Erikson, L., Hanson, H., 2004. An analytical model to predict dune erosion  
1733  
1734 642 due to wave impact. *Coastal Engineering*, 51, 675-696. DOI:  
1735  
1736 643 10.1016/j.coastaleng.2004.07.003  
1737  
1738  
1739 644 Link, L.E., 2010. The anatomy of a disaster, an overview of Hurricane Katrina and New  
1740  
1741 645 Orleans. *Ocean Engineering*, 37, 4-12. DOI: 10-1016/j.oceaneng.2009.09.002  
1742  
1743  
1744  
1745 646 Long, J.W., de Bakker, A.T.M., Plant, N.G., 2014. Scaling coastal dune elevation changes  
1746  
1747 647 across storm-impact regimes. *Geophysical Research Letters*, 41.  
1748  
1749 648 DOI:10.1002/2014GL059616  
1750  
1751  
1752 649 Masselink, G. and Hegge, B., 1995. Morphodynamics of meso and macrotidal beaches:  
1753  
1754 650 examples from central Queensland, Australia. *Marine Geology*, 129, 1-23. DOI:  
1755  
1756 651 10.1016/0025-3227(95)00104-2  
1757  
1758  
1759  
1760 652 Masselink, G., Scott, T., Poate, T., Russell, P., Davidson, M., Conley, D., 2016a. The  
1761  
1762 653 extreme 2013/2014 winter storms: hydrodynamic forcing and coastal response along  
1763  
1764 654 the southwest coast of England. *Earth Surface Processes and Landforms*, 41, 378-391.  
1765  
1766 655 DOI: 10.1002/esp.3836  
1767  
1768  
1769  
1770

1771  
1772  
1773 656 Masselink, G., Castelle, B., Scott, T., Dodet, G., Suanez, S., Jackson, D., Floc'h, F., 2016b.  
1774  
1775 657 Extreme wave activity during 2013/2014 winter and morphological impacts along the  
1776 Atlantic coast of Europe. *Geophysical Research Letters*, 43, 2135-2143. DOI:  
1777 10.1002/2015GL067492  
1778 659  
1779  
1780 660 Matias, A., Masselink, G., Turner, I., Williams, J.J., Ferreira, Ó., 2011. Detailed analysis  
1781 of overwash on gravel barriers. *Journal of Coastal Research*, SI 64, 10-14.  
1782  
1783 661  
1784  
1785 662 Matias, A., Williams, J., Masselink, G., Ferreira, O., 2012. Overwash threshold for gravel  
1786 barriers. *Coastal Engineering*, 63, 48-61. DOI: 10.1016/j.coastaleng.2011.12.006  
1787  
1788 663  
1789  
1790 664 Matias, A., Blenkinsopp, C.E., Masselink, G., 2014. Detailed investigation of overwash  
1791 on a gravel barrier. *Marine Geology*. 350, 27-38. DOI: 10.1016/j.margeo.2014.01.009  
1792  
1793 665  
1794  
1795 666 Matias, A., Masselink, G., Castelle, B., Blenkinsopp, C.E., Kroon, A., 2016.  
1796 Measurements of morphodynamic and hydrodynamic overwash processes in a large-  
1797 scale wave flume. *Coastal Engineering*, 113, 33-46. DOI:  
1798 10.1016/j.coastaleng.2015.08.005  
1799 669  
1800  
1801 670 Matias, A.. and Masselink, G., 2017. Overwash processes: lessons from fieldwork and  
1802 laboratory experiments. In: *Coastal Storms: Processes and Impacts*. Ed: Paolo Ciavola  
1803 and Giovanni Coco. John Wiley & Sons.  
1804 671  
1805  
1806 672  
1807  
1808 673 Mendoza, E.T. and Jiménez, J.A., 2006. Storm-induced beach erosion potential on the  
1809 Catalanian coast. *Journal of Coastal Research*, SI 48, 81-88.  
1810  
1811 674  
1812  
1813 675 Neumann, B., Vafeidis, A.T., Zimmermann, J., Nicholls, R.J., 2015. Future Coastal  
1814 Population Growth and Exposure to Sea-Level Rise and Coastal Flooding - A Global  
1815 Assessment. *PLoS ONE*, 10, e0118571.  
1816  
1817 676  
1818  
1819  
1820  
1821  
1822  
1823  
1824  
1825  
1826  
1827  
1828  
1829



1830  
1831  
1832 678 Nguyen, T.T.X., Bonetti, J., Rogers, K., Woodroffe, C.D., 2016. Indicator-based  
1833  
1834 679 assessment of climate-change impacts on coasts: A review of concepts, methodological  
1835  
1836 approaches and vulnerability indices. *Ocean and Coastal Management*, 123, 18-43.  
1837 680  
1838  
1839 681 DOI: 10.1016/j.ocecoaman.2015.11.022  
1840  
1841  
1842 682 Perini, L., Calabrese, L., Salerno, G., Ciavola, P., Armaroli, C., 2016. Evaluation of coastal  
1843  
1844 683 vulnerability to flooding: comparison of two different methodologies adopted by the  
1845  
1846 684 Emilia-Romagna region (Italy). *Natural Hazards and Earth Systems Science*, 16, 181-  
1847  
1848 194. DOI: 10.5194/nhess-16-181-2016  
1849  
1850  
1851 686 Poelhekke, L., Jäger, W.S, van Dongeren, A., Plomaritis, T.A., McCall, R., Ferreira, O.,  
1852  
1853 687 2016. Predicting coastal hazards for sandy coasts with a Bayesian Network. *Coastal*  
1854  
1855 688 *Engineering*, 118, 21-34. DOI: 10.1016/j.coastaleng.2016.08.011  
1856  
1857  
1858  
1859 689 Poulter, B. and Halpin, P. N., 2008. Raster modelling of coastal flooding from sea-level  
1860  
1861 690 rise. *International Journal of Geographical Information Science*, 22, 167-182.  
1862  
1863 691 DOI: 10.1080/13658810701371858  
1864  
1865  
1866  
1867 692 Ramirez, J.A., Lichter, M., Coulthard, T.J., Skinner, C., 2016. Hyperresolution mapping  
1868  
1869 693 of regional storm surge and tide flooding: comparison of static and dynamic models,  
1870  
1871 694 *Natural Hazards*, 82, 571-590. DOI: 10.1007/s11069-016-2198-z  
1872  
1873  
1874 695 Rodrigues, B. A., Matias, A., Ferreira, O., 2012. Overwash hazard assessment.  
1875  
1876 696 *Geologica Acta*, 10, 427-437. DOI: 10.1344/105.000001743  
1877  
1878  
1879  
1880 697 Roelvink, D., Reniers, A., van Dongeren, A.P., de Vries, J.V.T., McCall, R., Lescinski, J.,  
1881  
1882 698 2009. Modelling storm impacts on beaches, dunes and barrier islands. *Coastal*  
1883  
1884 699 *Engineering*, 56, 1133-1152. DOI: 10.1016/j.coastaleng.2009.08.006  
1885  
1886  
1887  
1888

1889  
1890  
1891  
1892  
1893  
1894  
1895  
1896  
1897  
1898  
1899  
1900  
1901  
1902  
1903  
1904  
1905  
1906  
1907  
1908  
1909  
1910  
1911  
1912  
1913  
1914  
1915  
1916  
1917  
1918  
1919  
1920  
1921  
1922  
1923  
1924  
1925  
1926  
1927  
1928  
1929  
1930  
1931  
1932  
1933  
1934  
1935  
1936  
1937  
1938  
1939  
1940  
1941  
1942  
1943  
1944  
1945  
1946  
1947

700 Sallenger, A.H., 2000. Storm impact scale for barrier islands. *Journal of Coastal*  
701 *Research*, 16, 890-895.

702 Sánchez-Arcilla, A., Jiménez, J.A., Peña, C., 2009. Wave-induced morphodynamic risks.  
703 Characterization of extremes. *Coastal Dynamics 2009*, World Scientific (CD), paper 127.

704 Sekovski, I., Armaroli, C., Calabrese, L., Mancini, F., Stecchi, F., Perini, L., 2015. Coupling  
705 scenarios of urban growth and flood hazards along the Emilia-Romagna coast (Italy).  
706 *Natural Hazards and Earth System Sciences*, 15, 2331-2346, DOI: 10.5194/nhess-15-  
707 2331-2015

708 Silveira, T.M., Taborda, R., Carapuço, M.M., Andrade, C., Freitas, M.C., Duarte, J.F.,  
709 Psuty, N.P., 2016. Assessing the extreme overwash regime along an embayed urban  
710 beach. *Geomorphology*, 274, 64-77. DOI: 10.1016/j.geomorph.2016.09.007

711 Smallegan, S.M., Irish, J.L., van Dongeren, A.R., den Bieman, J.P., 2016. *Morphological*  
712 *response of a sandy barrier island with a buried seawall during Hurricane Sandy.*  
713 *Coastal Engineering*, 110, 102-110. DOI: 10.1016/j.coastaleng.2016.01.005

714 Stockdon, H.F., Holman, R.A., Howd, P.A., and Sallenger, A.H., 2006. Empirical  
715 parameterization of setup, swash and run-up. *Coastal Engineering*, 53, 573-588.  
716 DOI: 10.1016/j.coastaleng.2005.12.005

717 Stockdon, H.F., Sallenger Jr, A.H., Holman, R.A., Howd, P.A., 2007. A simple model for  
718 the spatially-variable coastal response to hurricanes. *Marine Geology*, 238, 1-20.  
719 DOI:10.1016/j.margeo.2006.11.004

1948  
1949  
1950 720 Trifonova, E.V., Valchev, N.N., Andreeva, N.K., Eftimova, P.T., 2012. Critical storm  
1951  
1952 721 thresholds for morphological changes in the western Black Sea coastal zone.  
1953  
1954 722 *Geomorphology*, 143–144, 81–94. DOI:10.1016/j.geomorph.2011.07.036  
1955  
1956  
1957  
1958 723 Valchev, N., Andreeva, N., Eftimova, P., Prodanov, B., Kotsev, I., 2016. Assessment of  
1959  
1960 724 vulnerability to storm induced flood hazard along diverse coastline settings. *E3S Web*  
1961  
1962 725 *Conference 7*, 10002. FLOODrisk 2016 - 3rd European Conference on Flood Risk  
1963  
1964 726 Management.  
1965  
1966  
1967 727 van Koningsveld, M., Davidson, M.A., Huntley, D.A., 2005. Matching science with  
1968  
1969 728 coastal management needs: The search for appropriate coastal state indicators.  
1970  
1971 729 *Journal of Coastal Research*, 21, 399-411. DOI: 10.2112/03-0076.1  
1972  
1973  
1974  
1975 730 van Verseveld, H.C.W., van Dongeren, A.R., Plant, N.G., Jäger, W.S., den Heijer, C.,  
1976  
1977 731 2015. Modelling multi-hazard hurricane damages on an urbanized coast with a  
1978  
1979 732 Bayesian Network approach. *Coastal Engineering*, 103, 1-14. DOI:  
1980  
1981 733 10.1016/j.coastaleng.2015.05.006  
1982  
1983  
1984  
1985 734 Vousdoukas, M.I., Voukouvalas, E., Mentaschi, L., Dottori F., Giardino, A., Bouziotas, D.,  
1986  
1987 735 Bianchi, A., Salamon, P., Feyen, L., 2016. Developments in large-scale coastal flood  
1988  
1989 736 hazard mapping. *Natural Hazards Earth System Science*, 16, 1841-1853. DOI:  
1990  
1991 737 10.5194/nhess-2016-124.  
1992  
1993  
1994  
1995 738 Williams, J.J., Masselink, G., Buscombe, D., Turner, I., Matias, A., Ferreira, Ó., Metje, N.,  
1996  
1997 739 Coates, L., Chapman, D., Bradbury, A., Albers, A., Pan, S., 2009. BARDEX (Barrier  
1998  
1999 740 Dynamics Experiment): taking the beach into the laboratory. *Journal of Coastal*  
2000  
2001 741 *Research*, SI 56: 158-162.  
2002  
2003  
2004  
2005  
2006

2007  
2008  
2009  
2010  
2011  
2012  
2013  
2014  
2015  
2016  
2017  
2018  
2019  
2020  
2021  
2022  
2023  
2024  
2025  
2026  
2027  
2028  
2029  
2030  
2031  
2032  
2033  
2034  
2035  
2036  
2037  
2038  
2039  
2040  
2041  
2042  
2043  
2044  
2045  
2046  
2047  
2048  
2049  
2050  
2051  
2052  
2053  
2054  
2055  
2056  
2057  
2058  
2059  
2060  
2061  
2062  
2063  
2064  
2065

742 Wright, L.D. and Short, A.D., 1984. Morphodynamic variability of surf zones and  
743 beaches: a synthesis. *Marine Geology*, 56, 93-118. DOI: 10.1016/0025-3227(84)90008-  
744 2

2066  
2067  
2068  
2069  
2070  
2071  
2072  
2073  
2074  
2075  
2076  
2077  
2078  
2079  
2080  
2081  
2082  
2083  
2084  
2085  
2086  
2087  
2088  
2089  
2090  
2091  
2092  
2093  
2094  
2095  
2096  
2097  
2098  
2099  
2100  
2101  
2102  
2103  
2104  
2105  
2106

Table 1. Synthesis of process-based indicators by hazard, including calculation methods, input parameters, area of application and potential visual expression. OD – Overwash depth; OE – Overwash extent; FE – Flood depth; FD – Flood extent; SBR – Shoreline/berm retreat; DFR – Dune foot retreat; VE – Vertical erosion. The numbers in brackets refer to works where the indicators application/details can be found.

Hazard	Indicator	Method	Input parameters	Application [References]	Visual expression
Overwash	Overwash potential	Runup formulation (e.g. Holman, Stockdon)	Hs, Tp, sea level, beach face slope, dune crest height	Natural beaches/dunes [1-12]	Linear (along dune crest)
	Overwash depth	Runup formulation (e.g. Holman, Stockdon) + Donnelly formulation for depth decrease	Hs, Tp, sea level, beach face slope, dune crest height, backbarrier topography, overwash lens angle, backbarrier slope	Natural beaches/dunes/backbarriers [13-15]	2D with 3D possibility in association with OE
Inundation	Overwash extent	Numerical models (e.g. XBeach)	Nearshore wave conditions (Hs, Tp, direction); topo-bathymetry	Natural beaches/dunes/backbarriers [16, 17]	2D with 3D possibility in association with OE
		Donnelly Washover extent Formulation/XBeach	Hs, Tp, sea level, beach face slope, dune crest height, backbarrier topography, overwash lens angle, backbarrier slope/Nearshore wave conditions (Hs, Tp, direction); topo-bathymetry	Natural beaches/dunes/backbarriers [13-15, 18]	2D with 3D possibility in association with OD
	Flood depth/extent	Bathtub or tilted bathtub	Total sea level (tide + surge); Topography	Coastal areas with low morphological complexity [19-26]	2D with 3D possibility in association with FE/FD
	Flood depth/extent	Numerical models (e.g. LISFLOOD) or semi-static approaches	Water discharge/level; Topography	Low to complex hinterland morphologies [19, 24, 26]	3D
	Overflowing discharge volume	Numerical models (e.g. LISFLOOD) or semi-static approaches	Water discharge/level; Topography	Low to complex hinterland morphologies [19, 26]	3D

2107  
 2108  
 2109  
 2110  
 2111  
 2112  
 2113  
 2114  
 2115  
 2116  
 2117  
 2118  
 2119  
 2120  
 2121  
 2122  
 2123  
 2124  
 2125  
 2126  
 2127  
 2128  
 2129  
 2130  
 2131  
 2132  
 2133  
 2134  
 2135  
 2136  
 2137  
 2138  
 2139  
 2140  
 2141  
 2142  
 2143  
 2144  
 2145  
 2146  
 2147

Erosion	Shoreline/berm retreat; Dune foot retreat; Vertical erosion	Convolution model; Larson's model; Erosion structural function Numerical models (e.g. XBeach)	Nearshore wave conditions (Hs, Tp, direction); topo-bathymetry Nearshore wave conditions (Hs, Tp, direction); topo-bathymetry	Natural beaches/dunes [3, 13, 27-32] Natural beaches/dunes [16, 33-35]	SBR and DFR - 2D; VE - 3D SBR and DFR - 2D; VE - 3D
---------	-------------------------------------------------------------	--------------------------------------------------------------------------------------------------	----------------------------------------------------------------------------------------------------------------------------------	---------------------------------------------------------------------------	--------------------------------------------------------

[1] Almeida et al., 2012; [2] Armaroli et al., 2012; [3] Bosom and Jiménez, 2011; [4] Del Rio et al., 2012; [5] Duran et al., 2016; [6] Haerens et al., 2012; [7] Long et al., 2014; [8] Matias et al., 2014; [9] Rodrigues et al., 2012; [10] Silveira et al., 2017; [11] Stockton et al., 2007; [12] Trifonova et al., 2012; [13] Ferreira et al., 2016; [14] Christie et al., 2017; [15] Valchev et al., 2016; [16] Poelhekke, et al., 2016; [17] van Verseveld , et al., 2015; [18] Garcia et al., 2010; [19] Breilh et al., 2013; [20] Dottori et al., 2016; [21] Hinkel, et al., 2014; [22] Perini et al., 2016; [23] Poulter and Halpin, 2008; [24] Ramirez et al., 2016; [25] Sekovskii et al., 2015; [26] Vousedoukas et al., 2016; [27] Almeida et al., 2011; [28] Callaghan et al., 2008; [29] Ciavola et al., 2015; [30] Davidson et al., 2006; [31] Jiménez et al., 2016; [32] Mendoza and Jiménez, 2006; [33] McCall et al., 2010; [34] Smollegan et al., 2016; [35] van Verseveld et al., 2015.

2148  
2149  
2150  
2151  
2152  
2153  
2154  
2155  
2156  
2157  
2158  
2159  
2160  
2161  
2162  
2163  
2164  
2165  
2166  
2167  
2168  
2169  
2170  
2171  
2172  
2173  
2174  
2175  
2176  
2177  
2178  
2179  
2180  
2181  
2182  
2183  
2184  
2185  
2186  
2187  
2188

Table II. Comparison between computation type, longshore variability, comparability among coastal areas and cross-shore expression for selected geo, driver and process-based indicators.

Indicator type	Indicator name	Computation type	Longshore variability	Hazard comparability between coastal areas	Cross-shore hazard expression
Geoindicators	Shoreline position	DM/CE	Yes	Reduced	No
	Barrier/beach elevation	DM/CE	Yes	Reduced	No
	Beach/coastal slope	DM/CE	Yes	Reduced	No
	Erosion rate	CE/F/M	Yes	High	Yes
Driver-based indicators	Wave height	I/H	Reduced/Yes <sup>a</sup>	Reduced	No
	Tidal range	I/H	Reduced	Reduced	No
	Surge height	I/H	Reduced	Reduced	No
Process-based indicators	Overwash depth	F/M	Yes	High	Yes
	Overwash potential	F/M	Yes	High	No
	Overwash extent	F/M	Yes	High	Yes
Process-based indicators	Flood depth	F/M	Yes	High	Yes
	Flood extent	F/M	Yes	High	Yes
Process-based indicators	Shoreline/berm retreat	F/M	Yes	High	Yes
	Dune foot retreat	F/M	Yes	High	Yes
	Vertical erosion	F/M	Yes	High	Yes

<sup>a</sup> requires wave propagation models to include detailed longshore variability near the coastline;

DM – direct measurement; CE – cartographic extraction; I – instrumental; H – hindcast; F – formulation; M – model.